Scientific Reports

https://doi.org/10.1038/s41598-026-37673-x

Article in Press

Sustained release and efficacy of Kn2-7-loaded chitosan nanoparticles under low pH conditions

Received: 8 March 2025

Accepted: 23 January 2026

Published online: 05 March 2026

Cite this article as: Phathekile B., Sibuyi N.R.S., Meyer S. *et al.* Sustained release and efficacy of Kn2-7-loaded chitosan nanoparticles under low pH conditions. *Sci Rep* (2026). https://doi.org/10.1038/s41598-026-37673-x

Bonke Phathekile, Nicole Remaliah Samantha Sibuyi, Samantha Meyer, Abram Madimabe Madiehe, Grace Emily Okuthe, Martin Opiyo Onani & Mervin Meyer

Sustained release and efficacy of Kn2-7-loaded chitosan nanoparticles under low pH conditions

Bonke Phathekile[a], Nicole Remaliah Samantha Sibuyi[b,c*], Samantha Meyer[d], Abram Madimabe Madiehe[b,e], Grace Emily Okuthe[f], Martin Opiyo Onani[a*]and Mervin Meyer[b*]

[a]Organometallics and Nanomaterials, Department of Chemical Sciences, University of the Western Cape, Bellville, South Africa; [b]DSTI/TIA Nanotechnology Platform, Department of Biotechnology, University of the Western Cape, Bellville, South Africa; [c]Health Platform, Advanced Materials Division, Mintek, Randburg, Gauteng, South Africa; [d]Department of Biomedical Sciences, Cape Peninsula University of Technology; [e]Nanobiotechnology Research Group, Department of Biotechnology, University of the Western Cape, Bellville, South Africa; [f]Department of Biological and Environmental Sciences, Walter Sisulu University, Mthatha, South Africa

*Correspondence: NRSS – nsibuyi@uwc.ac.za; MOO – monani@uwc.ac.za; MM – memeyer@uwc.ac.za

ORCID: Bonke Phathekile - https://orcid.org/0000-0002-2097-0958
Nicole Sibuyi - https://orcid.org/0000-0001-7175-538
Samantha Meyer - https://orcid.org/0000-0002-5167-0608
Abram Madiehe - https://orcid.org/0000-0002-3935-467X
Grace E. Okuthe - https://orcid.org/0000-0001-6357-6742
Martin Onani - https://orcid.org/0000-0002-4735-3669
Mervin Meyer - https://orcid.org/0000-0002-8296-4860

Abstract

Delivery of antimicrobial peptides to low-pH sites is a significant challenge, and results in reduced treatment efficacy for vaginal infections. Chitosan nanoparticles (CNPs) could be ideal vehicles for drugs to acidic pH environments and sustain their therapeutic effects. CNPs were synthesized using the ionic gelation technique and loaded with Kn2-7 peptide. The CNPs were characterized by dynamic light scattering, Fourier transform infrared spectroscopy, high-resolution transmission and scanning electron microscopes. The stability and antibacterial effects of Kn2-7-loaded CNPs were evaluated at low and normal pH levels. The CNPs had a size distribution of 327-416 nm and a zeta potential of 9.61-23.9 mV. The size distribution (340.2-753.7 nm) and Zeta potential (15.9-67.7 mV) of CNPs changed after loading Kn2-7. The CNPs loading capacity and Kn2-7 entrapment efficiency were 35.6% and 78.3%, respectively. The Kn2-7-CNPs were not stable at low-pH and released Kn2-7 instantly; however, stabilization of Kn2-7-CNPs with poly (acrylic acid) (PAA) and tripolyphosphate (TPP) increased their stability and sustained Kn2-7 release at acidic pH. The Kn2-7-CNPs_1 mg/mL TPP-PAA inhibited the growth of *Staphylococcus aureus* at pH 3.8 better than the Kn2-7 alone. Therefore, the Kn2-7-CNPs_1mg/mL TPP-PAA could serve as a promising candidate for protecting and delivering drugs in low-pH environments.

Keywords: Antimicrobial peptides; Chitosan nanoparticles; Kn2-7 peptide; Microbicides; Sexually Transmitted Infections

1. Introduction

Many viruses can be transmitted from one person to the next during sexual contact or intercourse, examples include human immunodeficiency virus (HIV), human papillomavirus, hepatitis B, herpes, syphilis, chlamydia, and gonorrhea. Sexually transmitted infections (STIs) can cause long-term health problems, particularly in women and infants. The transmission of STIs can be prevented by the topical application of microbicides in the vagina or rectum before sexual intercourse [1]. Microbicides are promising tools for the prevention of STIs transmission [2], and could mitigate the spread of infections by eliminating these pathogens upon contact [1]. However, the acidic environment of the upper vagina, presents a challenge for many microbicidal agents [3], many of which are denatured at pH below 5 and neutralizing their antimicrobial activity [4]. Furthermore, cervical mucus acts as a barrier to the cervix, potentially impacting the distribution and effectiveness of microbicidal agents within the vagina and cervix [5], this renders the microbicides inefficient in the management and treatment of infectious organisms. There are various formulations of vaginal microbicides, including tablets, surfactants, films, gels, and ring microbicides. All of these formulations have failed in clinical trials due reduced bioavailability and stability, therefore high dosages will be required, which might induce adverse effects [6]. Therefore, it is postulated that nanomaterial-based delivery systems can help sustain the stability of these microbicides when used under low acidity and

high mucus content environments; to enhance their bioavailability and biodistribution in these hard-to-reach environments [7]. Nanomaterials with diameters of 1-1000 nm can effectively traverse mucus membranes, remain stable and accumulate in acidic environments, and allow for the controlled release of microbicidal agents. CNPs are among the organic nanomaterials that have been previously demonstrated to have mucus-penetrating properties [8], to be able to withstand acidic environments and degrade at a slower pace, thereby allowing slow release of their cargoes. This is a desirable attribute for drug delivery systems for application in harsh environments, to retain or enhance the activity of anti-STI agents.

Antimicrobial peptides (AMPs), whether synthetic or naturally derived, exhibit a wide range of activity against bacteria, fungi, and viruses. These naturally occurring host-defense peptides, produced by various organisms including bacteria, fungi, and plants, have garnered significant interest due to their antimicrobial properties and potential to combat drug-resistant microbes [9,10]. Kn2-7 [11] and human β-defensin3 (Hβd-3) [12] are examples of AMPs that have been shown to inhibit the growth of STIs, suggesting their potential use as microbicides. However, their susceptibility to degradation in acidic pH environments limit their application as microbicidal agents. CNPs emerge as nanocarriers of choice for delivery of AMPs in intravaginal sites and offer potential to develop more effective microbicides that are resistant to inactivation by low pH, can efficiently penetrate the mucus-rich vaginal environment and control release of the antimicrobial agents. The CNPs loaded with these peptides could, for example, be incorporated into a vaginal formulations and used as vaginal microbicides that can be topically applied within the vagina to prevent or treat microbial infections [13]. Therefore, the current research aimed to synthesize CNPs loaded with Kn2-7 (Kn2-7-CNPs) that are functional at low pH environments that simulate the vaginal environment. The stability and the prolonged release of Kn2-7 peptide were examined at acidic and basic pH. Additionally, the antibacterial effect of Kn2-7-CNPs against *S. aureus* at low and high pH levels were evaluated to determine their potential as a delivery system for antimicrobial agents for the prevention and treatment of vaginal infections.

2. Results and discussion

STIs have existed as long as humankind, and their treatment involves the use of microbicidal agents. Of the treatments involving the vaginal route, the major challenge arises from the vaginal environment, which is highly barricaded by the mucosal immune system. Delivery of microbicides in this environment poses a significant challenge due to biodegradation and an insufficient amount of drugs that reaches the organisms to kill the microbes. To achieve an adequate response, higher doses that are detrimental to the resident and surrounding cells may need to be used. NPs have demonstrated a massive role in transporting any type of drug to the target cells with reduced bystander effects [14], and have been explored as delivery vehicles for AMPs [10]. Among the organic nanomaterials, CNPs produced from a natural polysaccharide [15] has drawn medical attention as a drug delivery agent to cells that are part of mucosal membranes because of chitosan’s water solubility, muco- and bio-adhesive properties [16].

Chitosan and chitosan-based NPs could be ideal delivery agents for therapeutic agents in low pH environments, where they can be degraded slowly to release the drugs at the desired site and rate. The main advantage of chitosan over other equivalent drug delivery excipients is its favorable toxicological profile. Chitosan is commonly regarded as a non-toxic, non-irritant material and has been approved for use in cosmetics and as a food supplement in several countries [17]. This polymer is biocompatible and biodegradable and is widely used as a pharmaceutical excipient in a range of formulations such as powders, tablets, emulsions, and gels [18].

2.1. *Synthesis and characterization of Kn2-7-CNPs*

The KN2-7-CNPs were synthesized by cross-linking chitosan with TPP, and both the unloaded and AMP-loaded CNPs were stabilized with PAA as highlighted in Figure 1. The formation of the unloaded (CNPs) and Kn2-7-loaded CNPs (Kn2-7-CNPs) was also confirmed by SEM, and FTIR. Characterization of NP size and morphology is crucial for understanding their behavior and performance. DLS and HRTEM assess the physiochemical properties of NPs that provide complementary but distinct information: DLS measures the hydrodynamic diameter of particles in their solvated state, encompassing the core, any surface coatings, and the surrounding hydration layer. In contrast, HRTEM displays the core size and morphology of individual NPs, typically revealing the electron-dense material. DLS is also highly sensitive to the presence of aggregates, as these larger structures scatter light disproportionately, often leading to significantly larger diameters even if the primary particles core sizes are small [19].

2.1.1. DLS analysis

The light scattering effects and ζ-potential of free CNPs and Kn2-7-CNPs prepared using increasing concentrations of TPP are summarized in Table 1. The hydrodynamic diameters of the CNPs at 0.3 mg/mL, 1 mg/mL, and 2mg/mL of TPP were 327 nm, 416 nm, and 382 nm, respectively. This is consistent with findings by previous studies which demonstrated that the physical properties of CNPs are determined by the ratio of chitosan to TPP. These sizes were similar to the sizes of CNPs produced by crosslinking of chitosan with various di- and tricarboxylic acids (succinic acid, malic acid, tartaric acid, and citric acid) in a condensation reaction with 1-[3-(dimethylamino)propyl]-3-ethyl carbodiimide methiodide[20].

The PDI values of unloaded CNPs were between 0.293 and 0.592; while unloaded CNPs cross-linked with 2mg/mL of TPP and Kn2-7-CNPs crosslinked with 1 and 2 mg/mL TPP had PDI values of 0.341 and 0.365 and within ranges often associated with moderate colloidal stability (≤0.5). Stability can be challenged by environmental factors and subsequent coating processes [21–23]. The high Zeta potential values of the Kn2-7-CNPs indicated that they were least stable compared to unloaded CNPs. From the literature, only NPs with Zeta potentials within the +30 to -30 mV range are considered stable, this will help achieve AMP sustained release and prolonged residence time of the CNPs in acidic pH environments and mucosal sites. The DLS

suggested that the CNPs are polydispersed, which is based on the PDI values [24]. This observation could be attributed to the presence of two high-molecular-weight polymers (chitosan and TPP), as well as the effect of the freeze-drying process. It should also be noted that the Zeta potential for Kn2-7-CNPs-1mg/mLTPP was 54.3 mV, and it decreased to 37.2 mV after the CNPs were coated with PAA (Table 1). The PDI also increased from 0.341 to 0.840, which may be attributed to the presence of PAA, indicating significant polydispersity and increased aggregation, thereby reflecting less colloidal uniformity for the coated NPs.

2.1.2. HRTEM analysis

HRTEM analysis was used to examine the shape and core size distribution of CNPs. Figure 2 shows the varying sizes of CNPs and Kn2-7-CNPs at 1 mg/mL TPP. The CNPs micrograph (Figure 2a) showed mono-dispersed spherical NPs with a size range of 2 - 8 nm, while the Kn2-7-CNPs-1mg/mLTPP were polydispersed with various CNP shapes (Figure 2b). *T*he HRTEM for unloaded CNPs showed mono-dispersed spherical NPs, the Kn2-7-CNPs-1mg/mLTPP were polydispersed with various CNP shapes (Figure 2b), suggesting that both peptide loading and subsequent PAA coating contributed to morphological and size heterogeneity. Th*e* core size *wa*s significantly smaller than the hydrodynamic *size* measured by DLS, a disparity primarily explained by the fact that DLS measures solvated particles and their aggregates, while HRTEM only focus on the core [19]. The size difference strongly suggested the presence of NP aggregation in solution, even for the uncoated CNPs. Banerjee et al. [22], obtained spherical CNPs with a size or diameter range of 75 nm, 110 nm, and 50-600 nm using the ionic gelation method. The size differences depended on the amount of the crosslinker (glutaraldehyde) used, at 10%, 30%, and 100%, which clearly confirmed that the amount of the crosslinker influences the size of the CNPs. The shapes and sizes of CNPs can also be affected by their cargoes; the size usually increases after drug-loading. Dounighi et.al obtained spherical homogenous morphology of about 150 nm, the size increased to approximately 350 nm after loading scorpion venom into CNPs [23]. Past studies confirmed that hydrodynamic sizes at 300-700 nm range are indicative of the particles' behavior in solution, and suitable for biological applications, dictating interactions within the aqueous biological environment [25,26].

2.1.3. SEM analysis

SEM provides a direct picture of the surface and size information, and investigates the morphology of the test samples [27]. The SEM images for unloaded CNPs or CNPs_1mg/mLTPP (Figure 3a) showed spheroidal-shaped CNPs with smooth surfaces. The CNPs_1mg/mLTPP had a smaller size than the Kn2-7-CNPs (Figure 3b) and Kn2-7-CNPs_1mg/mLTPP (Figure 3c), possibly due to the loading of the peptide. Kiill et al reported on the CNPs crosslinked with TPP that had a spherical shape, smooth surfaces, and also a homogeneous particle size distribution in the range of 70 – 100 nm [28]. Hasheminejad and co-workers also reported on the spherical CNPs with sizes ranging between 129 - 148 nm, characterized by Field Emission SEM [29]. On the contrary, Amidi and co-workers reported that the loading of protein did not affect the size

and morphology of the CNPs [30]. The current study clearly demonstrated that loading the Kn2-7 peptide altered the properties of the CNPs and their morphology. The CNPs were successfully coated with PAA (Figure 3c) in the oval-shaped Kn2-7-CNPs with different layers shown by colored lines.

2.1.4. FTIR analysis

Figure 4 and Table 3 illustrate shifts and new peaks in the FTIR spectra of Kn2-7-CNPs_1mg/mLTPP-PAA compared to CNPs_1mg/mLTPP-PAA, indicating the presence of Kn2-7 and PAA. The absorption peak at 3033 cm^{-1} in the Kn2-7-CNPs_1mg/mLTPP-PAA spectrum corresponds to the O-H stretch from the carboxyl groups of PAA. The C-H stretching of the methyl group was observed at 2984 cm^{-1}. The decrease in the characteristic C=S peaks at 1645 and 1553 cm^{-1} coupled with the emergence of a new band at 1713 cm^{-1} suggests the presence of carboxyl groups from PAA. Furthermore, the broad peak at 2669 cm^{-1} confirms the presence of NH_3^+ in the Kn2-7-CNPs_1mg/mLTPP-PAA. The absorption peaks at 1453 and 1416 cm^{-1} are attributed to the asymmetric and symmetric stretching vibrations of the carboxylate anion (COO^-) groups, respectively. The peak at 1397 cm^{-1} corresponds to CH_2 groups, consistent with findings reported by Khan et al. in their research on PAA-chitosan hydrogels for targeted colon delivery [31]The shift of P=O peaks to 1260 and 1265 cm-1 was observed in both spectra, which confirmed that this coating did not affect the crosslinking. These results suggest that the carboxyl groups of PAA dissociated into carboxylate ions (COO^-), which then interacted electrostatically with the protonated amino groups of chitosan, forming a polyelectrolyte complex during the mixing process. The observed differences in exothermic peaks between the physical mixture and CNPs_1mg/mLTPP-PAA further support the formation of new chemical bonds upon coating Kn2-7-CNPs with PAA. These results suggested that the carboxyl groups of PAA dissociated into carboxylate ions (COO^-), which then interacted electrostatically with the protonated amino groups of chitosan, forming a polyelectrolyte complex during the mixing process. This interaction is key to PAA's role in stabilizing the NPs and mediating their pH-responsive and mucoadhesive properties relevant for vaginal delivery

2.1.5 Rationale for PAA Selection and Future Considerations

While PAA's advantages for controlled release and mucoadhesion in the vaginal environment are compelling, we acknowledge that the specific molecular weight of PAA used in this study (10000 Daltons) and the resulting coating thickness were not explicitly detailed or systematically optimized. These parameters significantly influence the steric stabilization, surface charge density, interaction with biological molecules, and subsequent behavior within mucosal barriers [26]. Although the large hydrodynamic diameters measured by DLS indirectly suggest a substantially hydrated polymer layer, direct quantitative measurements of coating thickness (via cryo-TEM or small-angle X-ray scattering) needs to be investigated for confirmation. The impact of the PAA coating on NP–mucus and NP–cell interactions is also required. PAA's mucoadhesive nature is beneficial for drug retention, but its interaction with

cellular surfaces (mediated by the altered zeta potential) needs further investigation to understand uptake mechanisms and potential cytotoxicity [32,33]. We recognize that a comprehensive understanding requires a systematic evaluation of these interactions. Future work will systematically investigate the influence of PAA molecular weight and coating density on the physicochemical properties, stability profile across varying pH conditions, and *in vitro* and *in vivo* biological performance of the Kn2-7-CNPs-PAA. Furthermore, comparative studies utilizing alternative biocompatible polymeric stabilizers like polyethylene glycol for “stealth” properties, or other mucoadhesive polymers would provide valuable insights into optimizing the formulation for enhanced antimicrobial efficacy and reduced side effects. This will allow for a more robust justification and selection of the optimal polymer for our delivery system.

2.2. %LC and %EE of Kn2-7 in CNPs

The Kn2-7 peptide was successfully incorporated into the CNPs, as shown by differences in the physicochemical properties of Kn2-7-loaded CNPs compared to those of free CNPs. The %EE and %LC values of Kn2-7-CNPs were 78.3% and 35.6%, respectively (Table 4). The %LC and %EE of Kn2-7 in the CNPs-TPP were more successful at 1 mg/mL of TPP, while 0.5 and 3mg/mL TPP showed poor loading and encapsulation efficiency of Kn2-7 peptide due to the competition between TPP and AMPs for the same positively charged sites on the chitosan [34].

2.3. Release of Kn2-7 peptide from Kn2-7-CNPs in different pH conditions

The stability of the Kn2-7-CNPs_1mg/mLTPP-PAA was evaluated to demonstrate how they will behave in different pH environments, particularly at low pH levels that simulate vaginal conditions. This test was done to determine how long the peptide will be retained inside the Kn2-7-CNPs_1mg/mLTPP-PAA before their release. This study will give an estimation of the residence time of the Kn2-7 peptide inside the CNPs at low pH, and the amount of the peptide that will be released over 24 hrs. In the current study, Kn2-7-CNPs_1mg/mLTPP-PAA was subjected to a pH of 3.8 and 4.2 for 24 hrs, and the Kn2-7 release profile was evaluated by quantifying its concentration using the Qubit protein assay kit. The CNPs were sonicated with no observation of any disintegration at the tested pH at baseline (0 hrs) (Table 5). This indicated that Kn2-7-loaded CNPs were stable in weak acids and basic environments. However, the Kn2-7 peptide was released immediately from the CNPs when subjected to low pH conditions for 24 hrs. The CNPs without PAA were not stable in the low pH range (3.8 and 4.2), when applying different actions (vortexing or incubation) to the CNPs at various time intervals.

An independent study demonstrated that mitomycin-C-loaded CNPs released mitomycin-C from the CNPs and sustained their release at pH levels of 6.0 and 7.4. The free drug was all released in 2 hrs, while release from CNPs was slower and lasted for 24 hrs at both pH [35]. Table 5 further demonstrates that the CNPs rapidly discharged their payload after being exposed to the low pH buffer and incubation for 24 hours, whether or not vortexing was performed, which is

contrary to the earlier study by Bhardwaj et al. [36]. Fathi et al. discovered that flurbiprofen-loaded CNPs had poor solubility at low pH, leading to poor drug release. However, they found that CNPs showed a rapid release of doxorubicin as the acidity increased. [37]. This research aimed to synthesize CNPs that are stable at low pH, ensuring prolonged and effective release of the AMP. The CNPs exhibited a burst release of Kn2-7 release within 1 hour at pH 3.8 and 4.2, followed by a slow release over 24 hours, with approximately 80% and 90%, respectively (Figure 5). The observed release curve indicated that the CNPs_1mg/mLTPP-PAA had a potential to release their cargoes in a pH-controlled and sustained rate. pH had a strong effect on drug release that followed the same trend at the two pH levels, that increased over timeand slightly higher at pH 3.8. Overall, drug release depended on both pH and time, with more release seen in more acidic conditions (pH 3.8).

2.5. Antibacterial activity of Kn2-7-CNPs

The low-pH stable Kn-2-7-loaded CNPs (Kn2-7-CNPs_1 mg/mLTPP-PAA) were assessed for their controlled and slow release of the AMP when subjected to low-pH environments that simulate the acidic vaginal environment. The growth kinetics of *S. aureus* at acidic conditions (pH 3.8) were not significantly different from those of the bacteria grown at normal pH (7.4) (data not shown). The Kn2-7-CNPs_1 mg/mLTPP-PAA showed better stability than the free AMP (Kn2-7 peptide) in acidic LB, and their antibacterial effect was evaluated on *S. aureus* cultured in high (7.4) and low pH (3.8) media. Kn2-7 AMP is a scorpion venom of that was derived from Buthus martensii Karsch [38], it has broad-spectrum antibacterial effects in both Gram-positive and Gram-negative bacteria [39] including the antibiotic-resistant strains such as *Escherichia coli*, *S. aureus,* and methicillin-resistant *Staphylococcus aureus* (MRSA) [11]. Studies have uncovered that this AMP exhibits a high level of anti-viral activity against HIV, making it a potential tool for preventing its transmission. Kn2-7 AMP inhibits microbial growth by direct interaction with microbes and is thus a promising drug candidate for the development of novel microbicidal agents [9,40] for intra-vaginal application to prevent the transmission of STIs. One of the significant challenges for treating STIs is that the intra-vaginal environment at a pH of 3.5 - 4.5 is very harsh and could degrade microbicides, leading to the loss of their antimicrobial activity. In the current study, CNPs were utilized as delivery agents for the Kn2-7 AMP to protect the AMP from rapid degradation in low-pH environments.

The bacterial activity of free Kn2-7 and Kn2-7-loaded CNPs was evaluated against *S. aureus* cultured in low (pH 3.8) and high (pH 7.4) pH environments. It should be noted that *S. aureus* served as a model organism to evaluate the ability of the CNP-PAA system to deliver and protect the activity of Kn2-7 within the low pH environment. The MIC values of Kn2-7 peptide (0 - 50 µg/mL), Kn2-7-CNPs_1mg/mL TPP-PAA (6.25 - 50 µg/mL), and the CNPs_1mg/mL TPP-PAA (0 - 12.5 µg/mL) were recorded after 24 hours. Table 6 shows that the free Kn2-7 peptide inhibited the growth of *S. aureus* at pH 7.4, with a MIC value of 6.25 µg/mL. The Kn2-7 peptide was reported to have a MIC value of 3.13 µg/mL against *S. aureus* cultured in pH of 7.4 normal

media [18]. In this study, the MIC value for Kn2-7 could not be established at pH 3.8, suggesting that the peptide's activity was affected by the low pH and failed to inhibit bacterial growth at concentrations up to 50 µg/mL. It is possible that the peptide was degraded entirely at the low pH and lost its antibacterial activity. The unloaded CNPs at concentrations ≤12.5 µg/mL did not exhibit any growth inhibitory effects against *S. aureus* at either pH 3.8 or 7.4. Interestingly, the CNPs loaded with the AMP (Kn2-7-CNPs, 1mg/mLTPP-PAA) demonstrated antibacterial activity at pH 3.8, indicating that the structure of the Kn2-7 peptide was retained even under low pH conditions

Kn2-7-CNPs_1mg/mLTPP-PAA had a MIC value of 6.25 µg/mL at pH 3.8 that was similar to the MIC value for Kn2-7 alone at pH7.4, this implied that the antibacterial activity of Kn2-7 was preserved at a low pH when loaded into the CNPs. Thus, the CNPs protected the Kn2-7 from degradation, which was confirmed by the antibacterial activity of Kn2-7 peptide at pH 3.8. The MIC for CNPs_1mg/mLTPP and CNPs_1mg/mLTPP-PAA could not be determined at the concentrations tested (≤ 12.5 ug/mL) and would require concentrations >12.5 µg/mL to induce a significant effect. This suggested that unloaded CNPs (CNPs_1mg/mL TPP-PAA) under the test conditions (both low and high pH) do not have any antibacterial activity against *S. aureus*, and that the antibacterial activity observed with the Kn2-7-CNPs_1mg/mLTPP-PAA was a result of the Kn2-7 peptide loaded onto CNPs_1mg/mL TPP-PAA. Bioactive CNPs have recently gained popularity as drug carriers and antimicrobial agents. Several researchers have studied the use of chitosan for vaginal delivery systems [41], and proven to have the ability to transport drugs, peptides, and proteins across mucosal barriers [42]. Interestingly, drug-loaded CNPs had improved the mucus diffusion efficiency of protein drugs such as insulin in diabetic rats and exhibited bioavailability that was 2.8-fold higher than that of unloaded CNPs [43]. The CNPs also ensured the controlled release of active antimicrobial agents, such as amoxicillin, from a chitosan nanocarrier compared to the commercial capsule [44]. The potential of the system to be used as a vaginal microbicide delivery system could be challenged by several factors that will delay its translation into clinical applications [33]. The colloidal stability of the nanocarriers must be improved by optimizing the nano-formulation to prevent early release and biodegradation of the drug. Testing against one strain (*S. aureus*) provides limited insight into the broad-spectrum efficacy required for a general vaginal microbicide. While *S. aureus* is a relevant pathogen, particularly given its increasing antibiotic resistance, a true microbicide platform would ideally demonstrate activity against a wider panel of clinically significant vaginal pathogens, including both Gram-positive and Gram-negative bacteria, as well as fungal and viral species. The relevance of this platform would also benefit from in vitro assays that will show their biocompatibility, mucus penetrating ability and interaction with human vaginal epithelial cells. Overall, the study demonstrated a critical step towards developing a vaginal microbicide by encapsulating Kn2-7 peptide within a CNP-based nanocarrier that is pH-dependent.

3. Conclusions

The current study showed that CNPs could serve as nanocarriers for Kn2-7 peptide, the AMP when encapsulated within the CNPs was protected from degradation and was delivered intact under low pH conditions. Thus, CNPs could be suitable nanocarriers for microbicides. CNPs-based microbicides can be used as topical vaginal gels or incorporated in a condom for protection and prevention against the transmission and spread of STIs. The CNPs demonstrated stability in low pH conditions, allowing for the modulated release of their encapsulated cargoes. The findings suggested that CNPs, as drug carriers, were able to enhance the *in vitro* release profile of Kn2-7 peptide, achieving a more controlled and sustained release. The antibacterial studies demonstrated that while free Kn2-7 is deactivated under acidic conditions, encapsulation within CNPs preserved its activity, even in simulated vaginal pH (approximately 3.8). The slow degradation of CNPs in this acidic environment enables the controlled release of the peptide, allowing it to exert its antibacterial effect. Encapsulating Kn2-7 peptide into CNPs protected the peptide from degradation in acidic conditions and preserved its antimicrobial activity. This suggested that CNPs_1mg/mLTPP-PAA may be an effective controlled delivery system for AMPs in acidic environments like the vagina. This approach holds promise for developing microbicidal products to prevent STIs. The mucus-penetrating ability of the Kn2-7-CNPs_1mg/mLTPP-PAA still needs to be tested on artificial mucus and monitored for its movement through the mucus and the time it takes to penetrate through the barrier. Their cytotoxicity effects and epithelial compatibility will be investigated in relevant vaginal models. The microbicidal activity and mechanisms of the Kn2-7-CNPs (1 mg/mLTPP-PAA) will further be investigated against a panel of clinically relevant microbes, additionally, *in vivo* studies will be used to determine if the CNPs can retain controlled release and prolong the residence time of Kn2-7 in animal studies.

4. Materials and Methods

4.1. *Synthesis of CNPs*

The synthesis of CNPs was carried out following an earlier approach as reported by Aminu Kura *et.al* [45] with some modifications. To prepare 2% chitosan solution, medium molecular weight chitosan (85% degree of deacetylation) (Sigma Aldrich, St Louis, MO, USA) was dissolved in 1% v/v acetic acid (Kimix, Cape Town, South Africa). The mixture was stirred with a magnetic stirrer at room temperature for 10 minutes. Different concentrations (0.3 – 5 mg/mL) of TPP (Sigma Aldrich) solution were added dropwise to the chitosan solution while stirring. The chitosan-TPP solution was sonicated on a Biobase UC-10SDII ultrasonic bath (Biobase Biodustry (Shandong) Co., Ltd., Jinan City, China) for 20 minutes, followed by centrifugation for 30 minutes at 14500 rpm in a mini spin AG 22331 Hamburg centrifuge (Eppendorf AG, Germany). The pellet was air-dried at room temperature.

4.2. *Synthesis of Kn2-7-loaded CNPs*

CNPs loaded with Kn2-7 peptide (Kn2-7-CNPs) were prepared according to the previous protocol [45]. A 0.5% chitosan solution was dissolved in 1% v/v acetic acid solution and stirred at room temperature for 10 minutes. Kn2-7 peptide (GL Biochem, Shanghai, China) was then added to the solution and stirred for another 15 minutes. TPP solution at 3 mg/mL was added to the Kn2-7/chitosan solution dropwise to form the Kn2-7-CNPs-TPP. The mixture was stirred for a further 30 minutes. The solution was then sonicated on a Biobase UC-10SDII ultrasonic bath for 20 minutes, followed by three washes in water and centrifugation as before. The pellets (Kn2-7-CNPs-TPP) were resuspended in water, then incubated at -20 °C. The frozen samples were freeze-dried using the Virtis freeze dryer (SP Scientific, Gardiner, NY, USA).

4.3. Stabilization of Kn2-7-CNPs-TPP with PAA

The Kn2-7-CNPs-TPP were coated with 1800 Da PAA (Sigma Aldrich) following the layer-by-layer (LBL) method described by Wu *et.al* [46]. The Kn2-7-CNPs-TPP (0.5 mg) were added to a 1 mL solution of 10 mg/mL PAA and stirred for 1 hour. The Kn2-7-CNPs_1mg/mLTPP-PAA mixture was then centrifuged at 14500 rpm at 37 °C for 30 minutes. The Kn2-7-CNPs_1mg/mLTPP-PAA were resuspended in 1 mL of milli-Q water, followed by ultra-sonication at 45 kHz for 20 minutes. The samples were frozen at -20°C and freeze-dried on the Virtis freeze dryer.

4.4. *Characterization of Kn2-7-CNPs*

The dynamic light scattering (DLS) technique was employed to investigate the size distribution, polydispersity index (PDI), and zeta potential of both free and loaded CNPs using a Nano ZS Zetasizer (Malvern Panalytical Ltd., Enigma Business Park, UK). The structural features of CNPs, Kn2-7-CNPs, and Kn2-7-CNPs_1mg/mLTPP-PAA were evaluated by FTIR-410® Jasco (Colchester, United Kingdom). The morphology and quality of the CNPs and Kn2-7-CNPs were investigated and captured by a Philips 400® high-resolution transmission electron microscope (HRTEM; The Netherlands) and Tescan MIRA3 RISE scanning electron microscopy (SEM; Tescan, China) at the Electron Microscope Unit (University of Cape Town, Rondebosch, South Africa).

4.5. *Loading efficiency of Kn2-7 on CNPs*

The loading capacity and encapsulation efficiency were determined using a method that was previously reported by Hussein-Al-Ali et. al [45]. The Kn2-7-CNPs _1mg/mLTPP-PAA obtained during synthesis in section 2.3 were aliquoted in 1.5 mL Eppendorf tubes and centrifuged for 1 hour at 14500 rpm. The supernatant was collected to quantify the amount of free Kn2-7 peptide, the absorbance was read at 210 nm on a Perkin Elmer Lambda 25 UV-visible spectrophotometer (Shelton, CT, USA). The encapsulation efficiency (%EE) and loading capacity (%LC) of the Kn2-7 peptide in the Kn2-7-CNPs _1mg/mLTPP-PAA were assessed by using the following equations (EQ) 1 and 2, respectively [45].

$$\text{EQ 1: \%LC} = \frac{A\text{Total peptide} - A\text{Free peptide}}{\text{NPs weight}} \times 100\%$$

$A_{\text{Total peptide}}$ = the absorbance of the free Kn2-7 equivalent to the amount of loaded encapsulation CNPs.

$A_{\text{Free peptide}}$ = the absorbance of the Kn2-7 in the supernatant of the CNPs.

NPs weight = the mass in mg of the CNPs that were used for loading the Kn2-7.

$$\text{EQ 2: \% EE} = \frac{A\text{Total peptide amount} - A\text{Free peptide}}{\text{Total peptide amount}} \times 100\% \text{ [47]}$$

A similar method was used to calculate %EE as in EQ 1, however, instead of dividing by the mass of CNPs, the amount of Kn2-7 in mg was used.

4.6. *Release of the Kn2-7 from CNPs*

The freeze-dried Kn2-7-CNPs and Kn2-7-CNPs_1mg/mLTPP-PAA were resuspended in phosphate-buffered saline (Sigma) at varying pH conditions (3.5 - 4.5 and 6.0 -7.4). An aliquot of 1 mL per sample was collected at 0 and 24 hours, the Kn2-7 peptide concentration was quantified in the supernatants using a Qubit™ Protein assay kit (Invitrogen, USA) following the manufacturer's instructions [48]. Briefly, 1µL of each sample, i.e., the CNPs (Kn2-7-CNPs and Kn2-7-CNPs_1mg/mLTPP-PAA) and increasing concentrations of bovine serum albumin as a standard, was individually mixed with 199 µL protein assay buffer and 1µL protein assay reagent. The samples were incubated in the dark at room temperature for 15 minutes. Kn2-7 peptide concentrations were obtained using a Qubit 2.0 fluorometer (Invitrogen).

4.7. Antibacterial activity of Kn2-7 and Kn2-7-CNP

4.7.1 Growth kinetics of S. aureus in low and high pH medium

The *S. aureus* strain was purchased from the American Type Culture Collection (Manassas, VA, USA). The bacteria were cultured using a microdilution assay as described elsewhere, with a few modifications [39]. Briefly, the bacteria were adjusted to a 0.5 McFarland turbidity standard in fresh Luria-Bertani (LB) at pH 7.4 (high) and pH 3.8 (low/acidic). The bacteria were plated at 10^6 CFU/mL without any treatments and cultured at 37 °C for 24 hours. Then, the growth rate of *S. aureus* at low and high pH conditions was assessed by measuring absorbance at 600nm every hour for the first 6 hours and at 24 hours using the POLARstar Omega microplate reader (Offenberg, Germany).

4.7.2. Determining the MIC of KN2-7 peptide and Kn2-7-CNPs

The Minimum Inhibitory Concentration (MIC) of KN2-7 peptide and Kn2-7-CNPs was evaluated on the *S. aureus* by a micro dilution assay as previously described [39], with some modifications. The *S. aureus* was cultured in LB at pH 3.8 and 7.4, and treated with Kn2-7, CNPs-PAA, and Kn2-7-CNPs_1mg/mLTPP-PAA. The CNPs-PAA and Kn2-7-CNPs_1mg/mLTPP-PAA were tested

at concentrations ranging from 1.56 to 25 µg/mL, while the Kn2-7 peptide was tested at concentrations ranging from 3.13 to 50 µg/mL. Ciprofloxacin (Sigma Aldrich) at 5 µg/mL was used as a positive control. The turbidity of the bacterial suspension was visually assessed after 24 hours of incubation at 37 °C as an indication of bacterial growth, and the absorbance was measured at OD 600nm on a POLARstar Omega microplate reader. The lowest concentration of the treatments that inhibited the visible growth of bacteria was recorded as the MIC.

4.8. Statistical analysis

The data was analyzed using two-way analysis of variance (ANOVA) through GraphPad Prism version 10.6.1 (Boston, MA, USA) for statistical analysis. Sidak's multiple comparisons post hoc test was employed when significant main effects or interactions were observed to determine specific differences between group means. Statistical significance was set at $p<0.05$ and the results are reported as mean ± standard deviation (SD) from 3 independent experiments performed in triplicate.

References

1. Rosenstein IJ, Stafford MK, Kitchen VS, Ward H, Weber JN, Taylor-Robinson D. Effect on Normal Vaginal Flora of Three Intravaginal Microbicidal Agents Potentially Active against Human Immunodeficiency Virus Type 1. J Infect Dis. 1998;177: 1386–1390. doi:10.1086/517820
2. Sánchez-Sánchez MP, Martín-Illana A, Ruiz-Caro R, Bermejo P, Abad MJ, Carro R, et al. Chitosan and Kappa-Carrageenan Vaginal Acyclovir Formulations for Prevention of Genital Herpes. In Vitro and Ex Vivo Evaluation. Mar Drugs. 2015;13: 5976–5992. doi:10.3390/md13095976
3. Lund P, Tramonti A, De Biase D. Coping with low pH: Molecular strategies in neutralophilic bacteria. FEMS Microbiol Rev. 2014;38: 1091–1125. doi:10.1111/1574-6976.12076
4. Nakano FY, Leão R de BF, Esteves SC. Insights into the role of cervical mucus and vaginal pH in unexplained infertility. Med Express. 2015;2: 1–8. doi:10.5935/MedicalExpress.2015.02.07
5. Hmed B, Serria HT, Mounir ZK. Scorpion Peptides: Potential Use for New Drug Development. J Toxicol. 2013;2013: 1–15. doi:10.1155/2013/958797
6. Notario-Pérez F, Ruiz-Caro R, Veiga-Ochoa MD. Historical development of vaginal microbicides to prevent sexual transmission of HIV in women: From past failures to future hopes. Drug Des Devel Ther. 2017;11: 1767–1787. doi:10.2147/DDDT.S133170
7. Cutler B, Justman J. Vaginal microbicides and the prevention of HIV transmission. Lancet Infect Dis. 2008;8: 685–697. doi:10.1016/S1473-3099(08)70254-8
8. Choudhury A, Das S, Kar M. A review on novelty and potentiality of vaginal drug delivery. Int J PharmTech Res. 2011;3: 1033–1044.
9. Lei J, Sun L, Huang S, Zhu C, Li P, He J, et al. The antimicrobial peptides and their potential clinical applications. 2019;11: 3919–3931.
10. Fadaka AO, Sibuyi NRS, Madiehe AM, Meyer M. Nanotechnology-based delivery systems for antimicrobial peptides. Pharmaceutics. 2021;13. doi:10.3390/pharmaceutics13111795
11. Chen Y, Cao L, Zhong M, Zhang Y, Han C, Li Q, et al. Anti-HIV-1 Activity of a New Scorpion Venom Peptide Derivative Kn2-7. 2012;7: 1–9. doi:10.1371/journal.pone.0034947
12. Inthanachai T, Thammahong A, Edwards SW, Virakul S, Kiatsurayanon C, Chiewchengchol D. The

Inhibitory Effect of Human Beta-defensin-3 on Candida Glabrata Isolated from Patients with Candidiasis. Immunol Invest. 2021;50: 80–91. doi:10.1080/08820139.2020.1755307

13. Pauwels R, De Clercq E. Development of vaginal microbicides for the prevention of heterosexual transmission of HIV. J Acquir Immune Defic Syndr Hum Retrovirology. 1996;11: 211–221. doi:10.1097/00042560-199603010-00001
14. Kumari P, Ghosh B, Biswas S. Nanocarriers for cancer-targeted drug delivery. J Drug Target. 2016;24: 179–191. doi:10.3109/1061186X.2015.1051049
15. Debi Prasanna M, Yogesh Panditrao Palve, Debasish Sahoo, Nayak PL. Synthesis and Characterization of Chitosan/Cloisite 30B (MMT) Nanocomposite for Controlled Release of Anticancer Drug Curcumin. Int J Pharm Res Allied Sci. 2012;1: 52–62.
16. Robertson J. 11119. Am Math Mon. 2004;111: 915. doi:10.2307/4145104
17. Qi L, Xu Z, Jiang X, Hu C, Zou X. Preparation and antibacterial activity of chitosan nanoparticles. 2004;339: 2693–2700. doi:10.1016/j.carres.2004.09.007
18. Kean T, Thanou M. Biodegradation , biodistribution and toxicity of chitosan ☆. Adv Drug Deliv Rev. 2010;62: 3–11. doi:10.1016/j.addr.2009.09.004
19. Filippov SK, Khusnutdinov R, Murmiliuk A, Inam W, Zakharova LY, Zhang H, et al. Dynamic light scattering and transmission electron microscopy in drug delivery: a roadmap for correct characterization of nanoparticles and interpretation of results. Mater Horizons. 2023;10: 5354–5370. doi:10.1039/d3mh00717k
20. Bodnar M, Hartmann JF, Borbely J. Preparation and characterization of chitosan-based nanoparticles. Biomacromolecules. 2005;6: 2521–2527. doi:10.1021/bm0502258
21. Honary S, Zahir F. Effect of Zeta Potential on the Properties of Nano-Drug Delivery Systems - A Review (Part 1). Trop J Pharm Res. 2013;12: 255–264.
22. Banerjee T, Mitra S, Kumar Singh A, Kumar Sharma R, Maitra A. Preparation, characterization and biodistribution of ultrafine chitosan nanoparticles. Int J Pharm. 2002;243: 93–105. doi:10.1016/S0378-5173(02)00267-3
23. N MD, Eskandari R, Zolfagharian H, Mohammad M. Preparation and in vitro characterization of chitosan nanoparticles containing Mesobuthus eupeus scorpion venom as an antigen delivery system. J Venom Anim Toxins Incl Trop Dis. 2012;18: 44–52. doi:10.1590/S1678-91992012000100006
24. Gimondi S, Ferreira H, Reis RL, Neves NM. Intracellular Trafficking of Size-Tuned Nanoparticles for Drug Delivery. Int J Mol Sci. 2024;25. doi:10.3390/ijms25010312
25. Vedantam P, Huang G, Tzeng TRJ. Size-dependent cellular toxicity and uptake of commercial colloidal gold nanoparticles in DU-145 cells. Cancer Nanotechnol. 2013;4: 13–20. doi:10.1007/s12645-013-0033-8
26. Hoshyar N, Gray S, Han H, Bao G. The effect of nanoparticle size on in vivo pharmacokinetics and cellular interaction. Nanomedicine. 2016;11: 673–692. doi:10.2217/nnm.16.5
27. Wang ZL. New developments in transmission electron microscopy for nanotechnology. Adv Mater. 2003;15: 1497–1514. doi:10.1002/adma.200300384
28. Kiilll CP, Barud H da S, Santagneli SH, Ribeiro SJL, Silva AM, Tercjak A, et al. Synthesis and factorial design applied to a novel chitosan/sodium polyphosphate nanoparticles via ionotropic gelation as an RGD delivery system. Carbohydr Polym. 2017;157: 1695–1702. doi:10.1016/j.carbpol.2016.11.053

29. Hasheminejad N, Khodaiyan F, Safari M. Improving the antifungal activity of clove essential oil encapsulated by chitosan nanoparticles. Food Chem. 2019;275: 113–122. doi:10.1016/j.foodchem.2018.09.085
30. Amidi M, Romeijn SG, Borchard G, Junginger HE, Hennink WE, Jiskoot W. Preparation and characterization of protein-loaded N-trimethyl chitosan nanoparticles as nasal delivery system. J Control Release. 2006;111: 107–116. doi:10.1016/j.jconrel.2005.11.014
31. Khan S, Anwar N. Highly Porous pH-Responsive Carboxymethyl Chitosan- Grafted -Poly (Acrylic Acid) Based Smart Hydrogels for 5-Fluorouracil Controlled Delivery and Colon Targeting . Int J Polym Sci. 2019;2019: 1–15. doi:10.1155/2019/6579239
32. Elfadil D, Elkhatib WF, El-sayyad GS, Nps A. Microbial Pathogenesis Promising advances in nanobiotic-based formulations for drug specific targeting against multidrug-resistant microbes and biofilm-associated infections. Microb Pathog. 2022;170: 105721. doi:10.1016/j.micpath.2022.105721
33. Chakraborty N, Jha D, Roy I, Kumar P, Gaurav SS. Nanobiotics against antimicrobial resistance : harnessing the power of nanoscale materials and technologies. J Nanobiotechnology. 2022; 1–25. doi:10.1186/s12951-022-01573-9
34. Grenha A, Seijo B, Remuñán-López C. Microencapsulated chitosan nanoparticles for lung protein delivery. Eur J Pharm Sci. 2005;25: 427–437. doi:10.1016/j.ejps.2005.04.009
35. Kavaz D, Kirac F, Kirac M, Vaseashta A. Low Releasing Mitomycin C Molecule Encapsulated with Chitosan Nanoparticles for Intravesical Installation. J Biomater Nanobiotechnol. 2017;08: 203–219. doi:10.4236/jbnb.2017.84014
36. Bhardwaj P, Singh S. Formulation and in vitro evaluation of ph-sensitive chitosan beads of flurbiprofen 1* 1. 2013;1: 48–54.
37. Fathi M, Zangabad PS, Majidi S, Barar J, Erfan-niya H, Omidi Y. Stimuli-responsive chitosan-based nanocarriers for cancer therapy. 2017;7: 269–277. doi:10.15171/bi.2014.008
38. Hui Zhang JW. Review on Bioactive Peptides and Pharmacological Activities of Buthus martensii Karsch. Biochem Pharmacol Open Access. 2015;04. doi:10.4172/2167-0501.1000166
39. Cao L, Dai C, Li Z, Fan Z, Song Y, Wu Y, et al. Antibacterial Activity and Mechanism of a Scorpion Venom Peptide Derivative In Vitro and In Vivo. 2012;7. doi:10.1371/journal.pone.0040135
40. Malcolm RK, Woolfson AD, Toner CF, Morrow RJ, Mccullagh SD. silicone elastomer vaginal rings. 2005; 954–956. doi:10.1093/jac/dki326
41. Tuğcu-Demiröz F, Saar S, Kara AA, Yıldız A, Tunçel E, Acartürk F. Development and characterization of chitosan nanoparticles loaded nanofiber hybrid system for vaginal controlled release of benzydamine. Eur J Pharm Sci. 2021;161. doi:10.1016/j.ejps.2021.105801
42. Zambito Y. Nanoparticles Based on Chitosan Derivatives. Adv Biomater Sci Biomed Appl. 2013; 243–263.
43. Liu M, Zhang J, Zhu X, Shan W, Li L, Zhong J, et al. Efficient mucus permeation and tight junction opening by dissociable “mucus-inert” agent coated trimethyl chitosan nanoparticles for oral insulin delivery. J Control Release. 2016;222: 67–77. doi:10.1016/j.jconrel.2015.12.008
44. Sahasathian T, Kerdcholpetch T, Chanweroch A, Praphairaksit N, Suwonjandee N, Muangsin N. Sustained release of amoxicillin from chitosan tablets. Arch Pharm Res. 2007;30: 526–531. doi:10.1007/BF02980229
45. Hussein-al-ali SH, Kura A, Hussein MZ, Fakurazi S. Preparation of Chitosan Nanoparticles as a

Drug Delivery System for Perindopril Erbumine. Polym Compos. 2016; 2–10. doi:10.1002/pc

46. Wu Y, Wu J, Cao J, Zhang Y, Xu Z, Qin X, et al. Facile fabrication of poly(acrylic acid) coated chitosan nanoparticles with improved stability in biological environments. Eur J Pharm Biopharm. 2017;112: 148–154. doi:10.1016/j.ejpb.2016.11.020
47. Saeed RM, Dmour I, Taha MO. Stable Chitosan-Based Nanoparticles Using Polyphosphoric Acid or Hexametaphosphate for Tandem Ionotropic/Covalent Crosslinking and Subsequent Investigation as Novel Vehicles for Drug Delivery. Front Bioeng Biotechnol. 2020;8: 4. doi:10.3389/FBIOE.2020.00004/BIBTEX
48. Id ZD, Olah Z, Id LM, Pakaski M, Galik B, Mihaly G, et al. Application of BisANS fluorescent dye for developing a novel protein assay. 2019; 1–8.

Author Contributions: SM, AMM, GEO, MOO and MM - Conceptualization, resources, supervision, funding acquisition; BP and NRSS - methodology, project administration, formal analysis, investigation and data curation; BP – writing-original draft preparation; NRSS, SM, AMM, GEO, MOO and MM – writing-review and editing. All authors have read and agreed to the published version of the manuscript.

Funding: This research was funded by NRF-Thuthuka Rating Track, Grant number TTK150625121238; UID: 99307 and UWC Natechnology platform.

Ethics declaration: Not applicable.

Data Availability Statement: The data presented in this manuscript can be requested from the corresponding authors on reasonable request.

Conflicts of Interest: The authors declare no conflict of interest.

Acknowledgments: The research data presented herein is part of Dr Bonke Phathekile's MSc project "Synthesis of peptide-loaded chitosan nanoparticles for the treatment of sexually transmitted infections (STI's), 2020" that is available on the university website.

Figure legends

Figure 1: Synthesis of PAA-stabilized Kn2-7-CNPs by the LBL technique [23].

Figure 2: HRTEM micrographs and size distribution of CNPs_1mg/mLTPP (a,c) and Kn2-7-CNPs_1mg/mLTPP (b,d), respectively.

Figure 3: SEM images for (a) CNPs_1mg/mLTPP, (b) Kn2-7-CNPs and (c) Kn2-7-CNPs_1mg/mLTPP-PAA (PAA = green, Kn2-7-CNPs = yellow).

Figure 4: FTIR spectra of (a) CNPs_1mg/mLTPP-PAA (b) Kn2-7-CNPs_1mg/mLTPP and (c) Kn2-7-CNPs_1mg/mLTPP-PAA.

Figure 5: Cumulative Kn2-7 peptide release profile from CNPs at pH 3.8 and pH 4.2 over 24 hours. Data are presented as mean ±SD, *$p < 0.05$, ****$p < 0.0001$.

Tables

Table 1: Particle size, PDI and Zeta potential of CNPs and Kn2-7-CNPs without PAA.

[TPP] (mg/mL)	% Chitosan		Particle size (nm)		PDI		Zeta potential	
	CNPs	Kn2-7-NCPs	CNPs	Kn2-7-CNPs	CNPs	Kn2-7-CNPs	CNPs	Kn2-7-CNPs
0.3	2	0.5	327.9±170.0	495.0±282.3	0.592±0.104	0.501±0.001	9.61±7.18	15.9±7.50
1	2	0.5	416.7±96.34	289.4±152.7	0.540±0.116	0.341±0.045	24.9±2.69	54.3±6.59
2	2	0.5	382.0±118.4	340.2±263.4	0.293±0.009	0.365±0.019	21.3±291	46.6±7.79

Table 2: Physico-chemical properties of Kn2-7-CNPs_1mg/mLTPP-PAA.

CNPs	Size (nm)	PDI	Zeta Potential (mV)
Kn2-7-CNPs_1mg/mLTPP-PAA	997±62.21	.840±0.043	+37.2±5.24

Table 3: FTIR results for CNPS, Kn2-7 CNPs.

Wavenumber		Vibration	Functional groups		Shift
Kn2-7-CNPs	Kn2-7-CNPs-PAA		Kn2-7-CNPs	Kn2-7-CNPs-PAA	
3400	3033	Stretching vibration	O-H, N-H	O-H, N-H	Yes
2929	2980	Asymmetric stretch	C-H	C-H	Yes
1643	1713	Bending vibration	COO^-	COO^-	New peak
1540	1453	Carbonyl stretch	CN	CN	Yes
1381	1376	Stretching	C-H (CH2), OH	C-H (CH2), OH	New peak
1226	1265	Stretching vibrations	P=O	P=O	Yes

Table 4: %EE and %LC values of AMP in the CNPs.

%EE	%LC

[TPP] mg/mL	Kn2-7-CNPs_1mg/mLTPP-PAA	Kn2-7-CNPs_1mg/mLTPP-PAA
0.3	50.7±0.819	38.3±0.603
1	78.3±0.603	35.6±0.361
3	55.6±0.850	46.9±1.601

Table 5: Stability of Kn2-7-CNPs_1mg/mLTPP-PAA in different pH conditions.

pH	Time (hrs)	Temperature	[Kn2-7] µg/mL
3.8	0	Room temperature	0
3.8	24	37 °C	48
4.2	0	Room temperature	0
4.2	24	37 °C	53.2

Table 6: MIC values as a measure for anti-bacterial activity of Kn2-7 and Kn2-7-CNPs_1mg/mL TPP-PAA.

Parameters	Kn2-7		CNPs_1mg/mLTPP-PAA	Kn2-7-CNPs_1mg/mLTPP-PAA
pH	7.4	3.8	3.8	3.8
MIC (µg/mL)	6.25	>50	>12.5	6.25

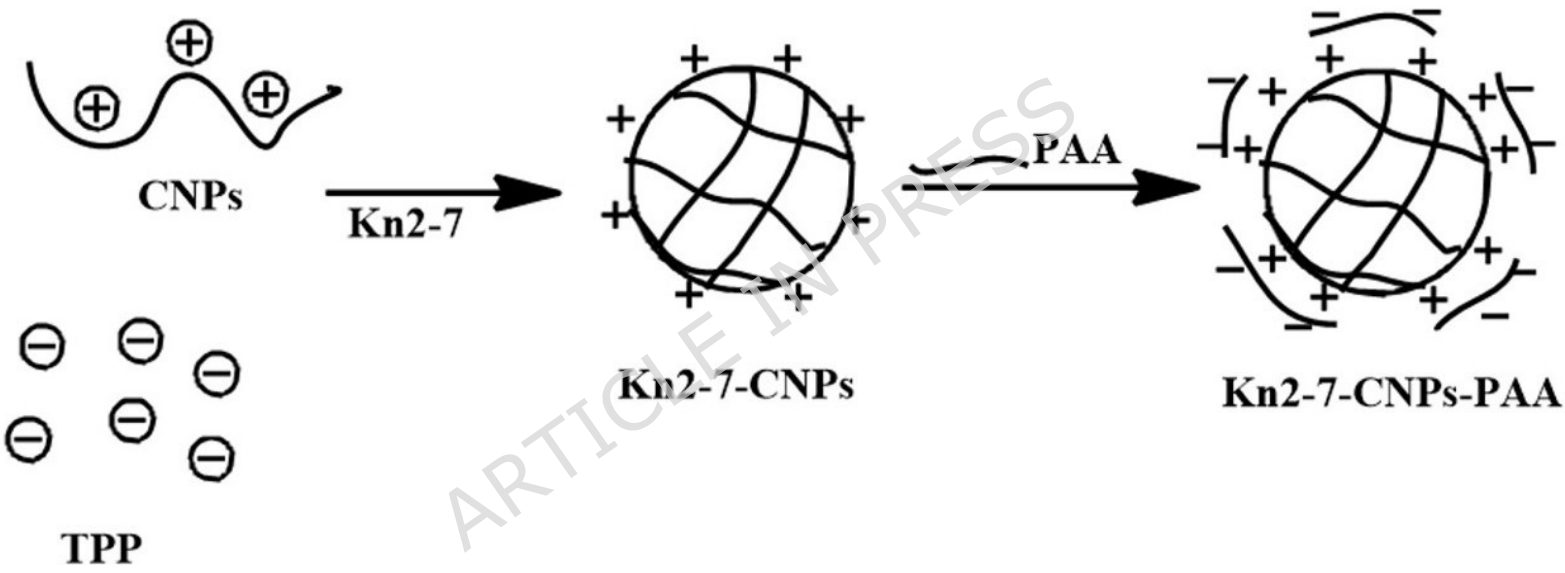

(a)

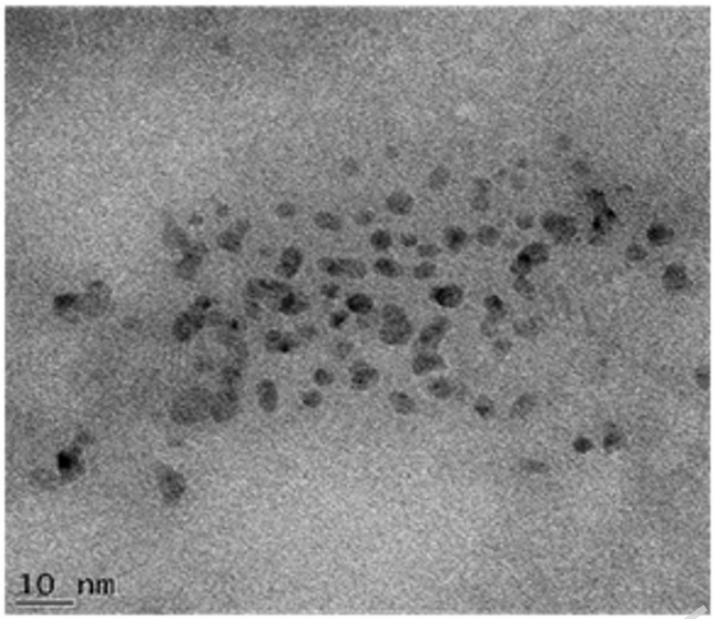

(b)

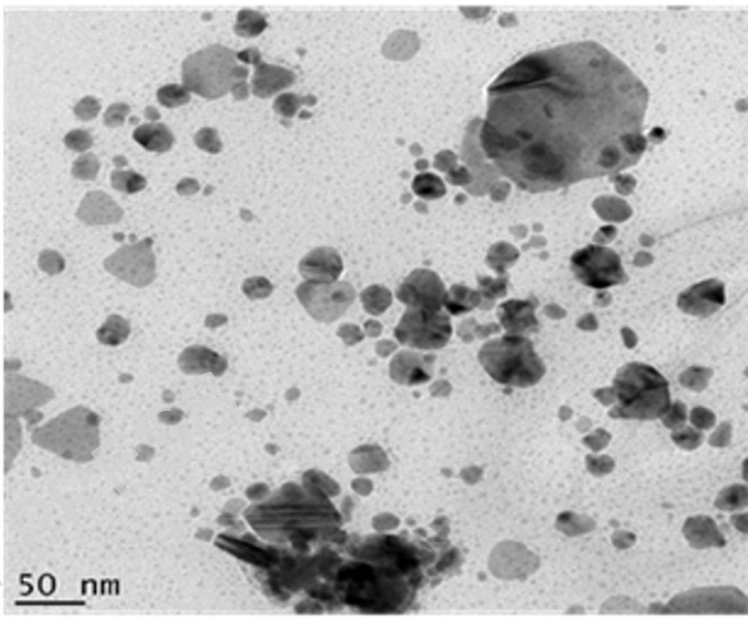

(c)

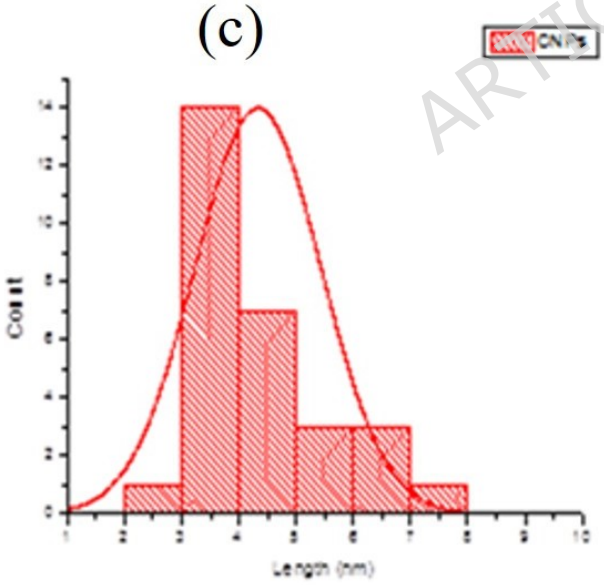

(d)

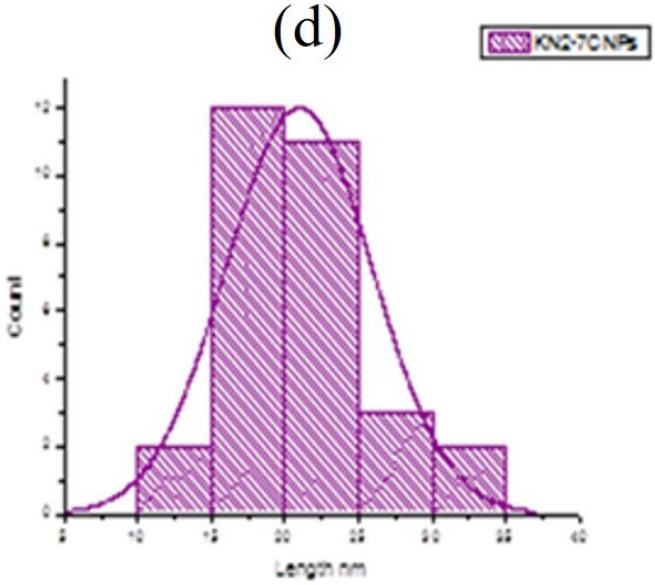

(a) (b) (c)